Significance of Morphological Features in Rice Variety Classification Using Hyperspectral Imaging

Vladan Filipović
Biosense Institute
University of Novi Sad
Novi Sad, Serbia
vladan.filipovic@biosense.rs

Marko Panić
Biosense Institute
University of Novi Sad
Novi Sad, Serbia
panic@biosense.rs

Sanja Brdar
Biosense Institute
University of Novi Sad
Novi Sad, Serbia
sanja.brdar@biosense.rs

Branko Brkljač
Faculty of Technical Sciences
University of Novi Sad
Novi Sad, Serbia
brkljacb@uns.ac.rs

2021 12th International Symposium on Image and Signal Processing and Analysis (ISPA) | 978-1-6654-2639-8/21/$31.00 ©2021 IEEE | DOI: 10.1109/ISPA52656.2021.9552086

Varietal classification of rice seeds is a crucial task in the process of rice crop production, management, and quality control. Traditionally, classification is performed manually which gives slow and inconsistent results. Machine vision technology provides an automated, real-time, non-destructive and cost-effective solution to this problem. Methods that combine RGB and hyperspectral imaging have shown very good results in rice seed classification. In this paper, we demonstrate the significance of morphological and border related features used in addition to spectral information and propose a feature set that provides a substantial improvement in classification results. The proposed approach was successfully tested on a publicly available dataset of 8640 seed samples corresponding to 90 different rice seed varieties, contained in 180 hyperspectral and RGB image pairs, and resulted in an average F1 score of 85.65%.

Keywords—automated inspection, morphological features, rice seed classification, hyperspectral imaging, contour features

I. Introduction

Rice (Oryza sativa) is a staple food crop for more than 50% of the world's population, with the majority of rice consumption occurring in developing nations [1]. As rice is one of the most frequently grown crops in a number of countries, many different species have been developed with the aim of being resistant to different environmental conditions, as well as to achieve the desired flavor and nutritional values [2]. In rice seedling nurseries and propagation stations, significant efforts are being made to prevent varietal contamination in order to eliminate variety impurities and mutations that may adversely affect crop quality [3]. Seedling propagation stations and plant protection centers traditionally employ professional inspectors who use standard methods of manual classification based on shape and color. This process is non-efficient and time-consuming and it allows for inconsistent classification due to fatigue, bad lighting conditions and inspector subjectivity [4], [6]. Real-time, reliable and non-destructive method of automation of this process would enable more efficient distribution of human resources while producing fast and consistent results.

In order to develop a real-time and reliable automatic system for rice classification, the following approaches are reported in literature: extraction of morphological and textural features from RGB images [3], extraction of spectral features from hyperspectral images [2] or combination of these two feature sets [6]. Besides relying on hand-crafted feature sets, other approaches include deep learning techniques [3], [4].

A large number of publications describe experiments done with classifiers trained to differentiate among less than 15 varieties of rice seeds [2-4], [6], [7]. Such classifiers are not suitable for a practical application in an industry that involves cultivation of hundreds of rice seed varieties. Furthermore, experiments are often done on datasets that are not publically available, which prevents transparent testing of new classification models. A more detailed overview of current publications with description of used methods, number of varieties and achieved results is given in [8].

In this paper, a new set of features is proposed for improving the classification of a large number of rice seed varieties using RGB and hyperspectral imaging. The primary focus of the analysis are the applicability and the performance of a new set of morphological and border related features. Proposed spatial domain features proved to provide useful information for better discrimination among selected 90 seed varieties that exhibit great similarities in different seed shape attributes. Thus, although the classification based only on spatial domain features is very challenging, further improvements were made in comparison to previous approaches proposed in the literature. Specifically, the design of the new feature set is the result of the proposed improvements in the following domains:

- Uneven illumination of rice seeds is corrected for more consistent segmentation of their regions from the background.
- A new set of spatial features based on morphological and border related attributes that provide capabilities for better discrimination among a large number of rice seed varieties is proposed.
- The mean of spectral responses for each seed, as a spectral feature, is further extended by introducing the variance of spectral responses.
- A better approach for dimensionality reduction is proposed using the neighborhood component analysis (NCA) on a full set of features.

Listed improvements were confirmed through comprehensive and detailed numerical experiments based on the publicly available image dataset described in [8], available at [9], consisting of high resolution hyperspectral and RGB images corresponding to 90 different rice seed varieties.

The paper is organized as follows. In section II a description of the used dataset is given and all preprocessing, feature extraction and dimensionality reduction steps utilized in the experiments are explained. Section III presents

The authors acknowledge the support of the Ministry of Education, Science and Technological Development of the Republic of Serbia (No. 451-03-9/2021-14/200358) and HARMONIC project. This work was partially supported from the European Union's Horizon 2020 research and innovation programme under grant agreement No. 810775 (DRAGON).

experimental results and performance evaluation of the proposed techniques and improvements, while section IV concludes the work and suggests future research directions.

II. Methods

A. Dataset Description

The dataset contains 90 varieties of rice seeds with 96 samples (seeds) per variety. Samples of each variety are imaged in two bundles of 48 seeds, distributed in 6 by 8 grids on a black background plate. Imaging is done simultaneously with RGB and a hyperspectral camera. RGB camera has a resolution of 4896 by 3264 pixels. The used hyperspectral camera is a VIS/NIR (visible/near-infrared) camera capturing reflectance in the range from 385 nm to 1000 nm on 256 discrete wavelengths. For dark and white references, a shutter and a white spectralon surface, respectively, were used, and pseudo-absorbance was calculated. Reflectance standards are essential for image calibration, to correct pixel-to-pixel variations arising due to inconsistencies in capture and illumination of samples [15].

Besides the mentioned 180 RGB images and hyperspectral data cubes, the dataset also contains an image of the chessboard pattern that is used for correction of spatial and lens distortion effects. Imaging setup and dataset are described in more detail in [8]. The dataset is publicly available at [9].

B. RGB image Preprocessing and Rice Seed Segmentation

In order to get consistent and precise spatial regions corresponding to individual rice seeds in each RGB image, several independent preprocessing steps were utilized. At the end, seed segmentation binary masks were obtained by thresholding of the red channel of RGB images.

In the first stage, the preprocessing was related to the elimination of the lens distortion effects. Lens distortion correction was performed using the approach described in [10]. A checkerboard pattern image provided with the dataset was used to estimate the required transformations for radial, decentering and thin prism distortions.

The second preprocessing step was related to the elimination of illumination inconsistencies. It consisted of applying a suitable image transform in order to achieve uniform illumination intensity across the whole image. In the described imaging setup light source was positioned in a way that did not provide uniform illumination over the entire imaged area, as shown in Fig. 1. E.g. light intensity on the obtained RGB images is noticeably greater on the side closer to the light source. Therefore, illumination correction using the approach described in [11] was needed as the second preprocessing step. The variable light intensity over the acquired region is modeled using a linear gradient. The illumination gradient was estimated using linear regression and the corrected image was obtained by subtracting the gradient from the original image, as shown in Fig. 1.

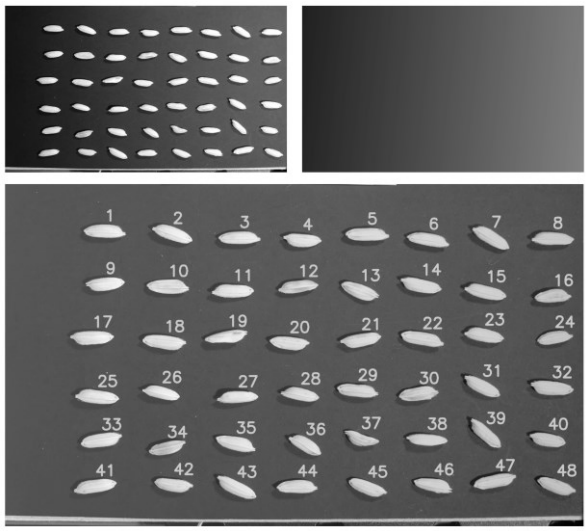

Fig. 1. Illumination gradient correction: original image (top left), estimated illumination gradient (top right) and corrected image with seed labels (bottom)

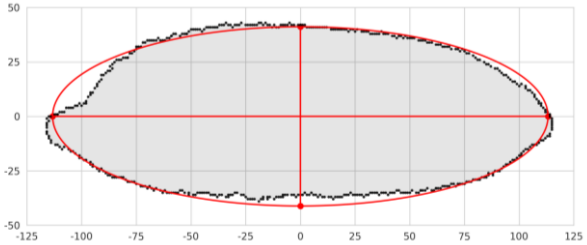

Fig. 2. Extraction of the standard feature group: seed region diagram, ellipse with the same normalized second central moment, major and minor axes

After applied corrections aimed at spatial and illumination distortions caused by the imaging setup and camera imperfections, seed region binary masks were obtained by thresholding of the red channel. The threshold value was selected heuristically. Histograms were plotted for a subset of images belonging to randomly selected classes and the initial value was selected. The value was then adjusted to provide satisfactory seed border precision for all given images. Reflective particles were eliminated on the basis of the surface area of their regions, which is noticeably smaller than the surface area of the seed (ranging from 8000 to 22000 pixels). Other reflections and non-seed regions were eliminated on the basis that their irregular shape results in solidity values much smaller than in the seed regions. In this way it was ensured that only 48 seed regions remained masked.

The placement of seeds in 6 by 8 grids enables a consistent labeling scheme for all images. Seed region centroid coordinates are sorted by both axes and used to label seeds in left-to-right and top-to-bottom order, as shown in Fig. 1. This deterministic labeling scheme enables quick and easy seed identification which is useful when combining multiple imaging modalities (RGB and hyperspectral). It also enables analysis of the impact of seed placement on classification results, which can be an indicator of non-uniform lighting and spatial distortion.

C. Spatial Feature Extraction

In this section we elaborate on the five groups of features that are based on different approaches to seed shapes description. In this paper, the focus was only on features that are invariant to translation and rotation of rice seeds in order to make a robust and reliable classifier.

1) The original group of seed region properties (the baseline spatial description)

This group of features is shown to be effective for discrimination among species and is often used as a basic seed shape description (set of spatial features) in addition to the spectral features [6], [8]. It consists of six features, beginning with seed region area and perimeter over the area ratio. The

next four features are based on an ellipse that has the same normalized second central moment as the seed region, as illustrated in Fig. 2. These features are major axis length, minor axis length, aspect ratio (ratio of minor to major axis length) and eccentricity (ratio of the distance between two foci to the major axis length).

In addition to the previous group of 6 baseline features, the next 4 groups of rice seed spatial features are newly proposed and provide information about additional spatial attributes.

2) Additional seed region features

This group contains nine features related to the first group but different enough to provide more of the discriminative information needed to differentiate between greatly similar seed shapes. These are seed region perimeter, convex area, solidity (ratio of area to convex area), equivalent diameter (diameter of a circle with the same area as the seed region), compactness, circularity, roundness and symmetry over major and minor axes. Compactness and circularity were defined in [12]. Roundness is often calculated in different ways, but here it is defined as a ratio of the minimal and maximal distance from the seed region centroid to its border, illustrated in Fig. 3. Symmetry over axes is defined as the intersection over union (IoU) of the seed region area with itself after the seed region area is folded in half over the selected axis.

The next three groups of features are based on different methods of describing the seed region border. They require morphological opening to be applied to seed region binary masks in order to make them smoother and enable a more consistent border description.

3) Border distance features

As the name suggests this group of features is based on the distance of the seed region border points to the centroid. It contains minimal and maximal distance and a set of statistical properties describing the distribution of these distances: mean value, standard deviation, variance, third and fourth moment, three quartiles, skewness and kurtosis. In total, 12 statistics.

An array of border distances can be regarded as a period of an infinite periodic function, which makes it suitable for analysis using FFT (fast Fourier transform) [16]. For that reason, the extracted array of border distances is used to define the border distance function which is then resampled in 512 points to make the usage of the FFT algorithm more efficient. Out of the 512 FFT coefficients obtained this way, the first 20 coefficients corresponding to the low frequency range proved to be the most informative and their amplitudes (moduli) were used as features. Although the border distance function depends on the starting point at the seed border, using only amplitude information and discarding phase information ensures invariance to seed rotation. In total, there are 32 border distance features.

4) Border signature features

Further, the contour of the seed region is described using distance from the centroid to the boundary as a function of an angle. The border signature is described in [12] and illustrated in Fig. 3. This group of features is similar to the previous group, excluding minimum and maximum to avoid repetition. A set of 10 statistical properties is calculated, along with the amplitudes of the first 20 FFT coefficients, which in total gives 30 border signature features.

5) Slope chain code related features

The slope chain code (SCC) requires the border shape to be approximated by placing straight-line segments of equal length around the curve, with the end points of the segments touching the curve, as shown in Fig. 4. SCC consists of an array of normalized slope changes between said segments. Tortuosity is defined as the sum of absolute values of the SCC chain elements, and it is a measure of border wiggle. Concepts and definitions of SCC (slope chain code) and tortuosity are given in [12]. This feature group contains the seed border tortuosity and statistical properties of SCC, same as the previous two feature groups. SCC values depend on the position of the starting point for seed border approximation, however the statistical properties of SCC are invariant under rotation.

D. Spectral Preprocessing and Feature Extraction

Extracting data from hyperspectral images also requires a preprocessing step to reduce variation in the reflectance due to the acquisition setup. To get consistent and unbiased spectral features, hyperspectral images were corrected using the standard approach, utilizing provided black and white reference images [8].

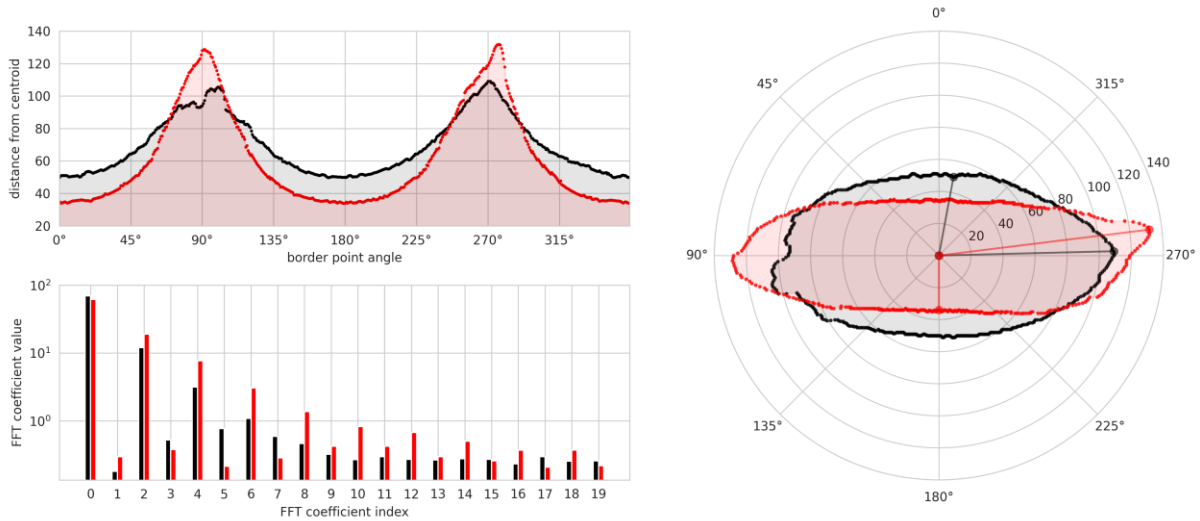

Fig. 3. Proposed border signature features illustrated on two seed samples (denoted by red and gray color). Border signature function (top left), first 20 coefficients of border signature FFT (bottom left), seed region diagram and distances used to calculate roundness (right). Ten additional statistical features describing distribution of border signature values from this group of features are not shown in the figure.

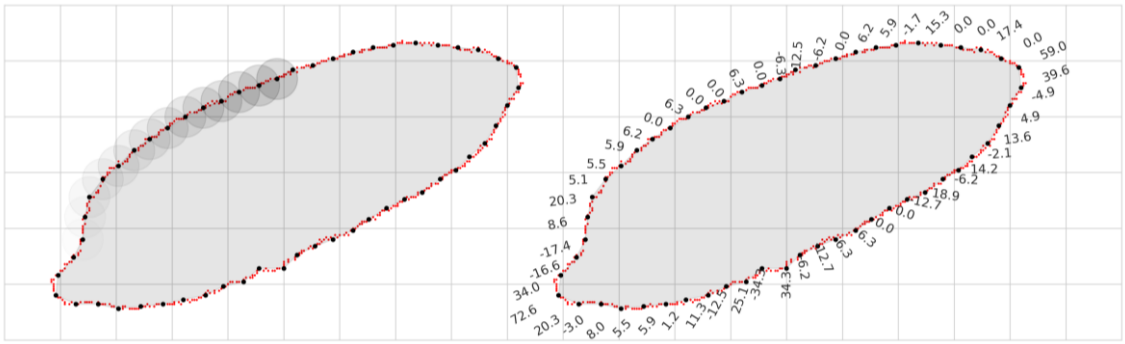

Fig. 4. The process of generating slope chain code. Left: contour approximation using 9 pixel long segments. Right: angles of slope changes between adjacent segments. Angles are calculated in degrees and later divided by 180 to obtain slope change codes.

After correction, it was estimated that 7 channels of the hyperspectral image in the range from 667 nm to 681 nm exhibit the greatest difference in value between seed regions and the background plate. Therefore, in order to obtain the final seed region binary masks based on the heuristic thresholding approach described in section II-B, for each hyperspectral image a grayscale image was created by spectral averaging of selected hyperspectral channels. This differs from the approach used in [8] and enables seed region masks to be adapted in order to maximize segmentation and classification results. Seed masks obtained from RGB and hyperspectral images are labeled using the same labeling scheme, which enables easy management of data extracted from different imaging modalities.

The baseline feature set extracted from hyperspectral images includes only the mean reflectance value of the seed region for each available wavelength [8], [7], i.e. the feature vector corresponding to the average spectral signature of all seed pixels. This approach does not ensure maximal utilization of the information provided by hyperspectral imaging. In this paper, we extended the spectral feature set by adding the variance of pixels' reflectance for each wavelength.

E. Dimensionality Reduction

Described feature extraction utilized in this study results in two feature sets: 1) the morphological set containing 88 features, and 2) the spectral set containing 512 features. Many subsets of these features are highly correlated because they are based on similar properties of seed shapes in the case of morphological features or reflectance at close wavelengths in the case of spectral features. A large number of features and substantial correlation among them are reasons to adopt feature elimination or dimensionality reduction.

Three forms of dimensionality reduction were analyzed: feature elimination based on mutual information (MI) score, recursive feature elimination (RFE) and neighborhood component analysis (NCA). Mutual information is a measure used in information theory to estimate the degree of mutual dependence between two random variables [17]. Applied here, it measures the amount of information obtained about seed class labels through the observation of the selected feature. Eliminating features based on MI assures that only features which are the most informative for discrimination among the given 90 classes are used for classification. The second form of feature elimination, RFE, involves training a classifier in multiple iterations and eliminating a certain number of features that are estimated to be least informative in every iteration. The third method, NCA, is a supervised dimensionality reduction technique that aims to find a linear transformation of input feature space such that the average leave-one-out classification performance is maximized in the transformed space [13]. NCA can be initialized using standard techniques like linear discriminant analysis (LDA) and principal component analysis (PCA).

F. Rice Seed Variety Classifier

One of the main objectives that we address in this paper is the creation of an informative and robust morphological feature set which will be used together with hyperspectral features for rice seed classification. In order to demonstrate the gains achieved by using the new morphological feature set, we create two rice classification schemes: 1) using the morphological feature set alone and 2) using it in combination with spectral features.

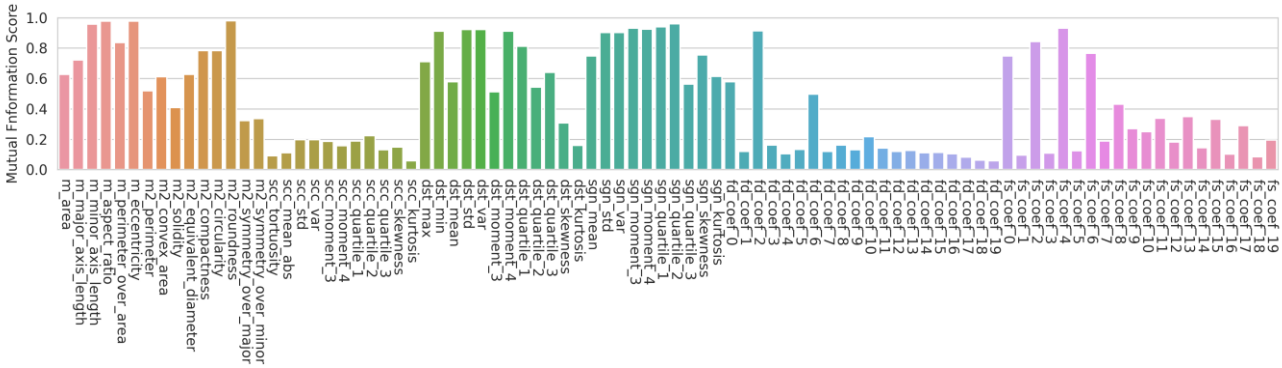

Fig. 5. Mutual information score as a measure of feature importance. The feature group is indicated in the prefix of the feature name. Feature groups in left-to-right order: standard morphological, additional morphological, SCC, border distance, border signature, border distance FFT and border signature FFT features

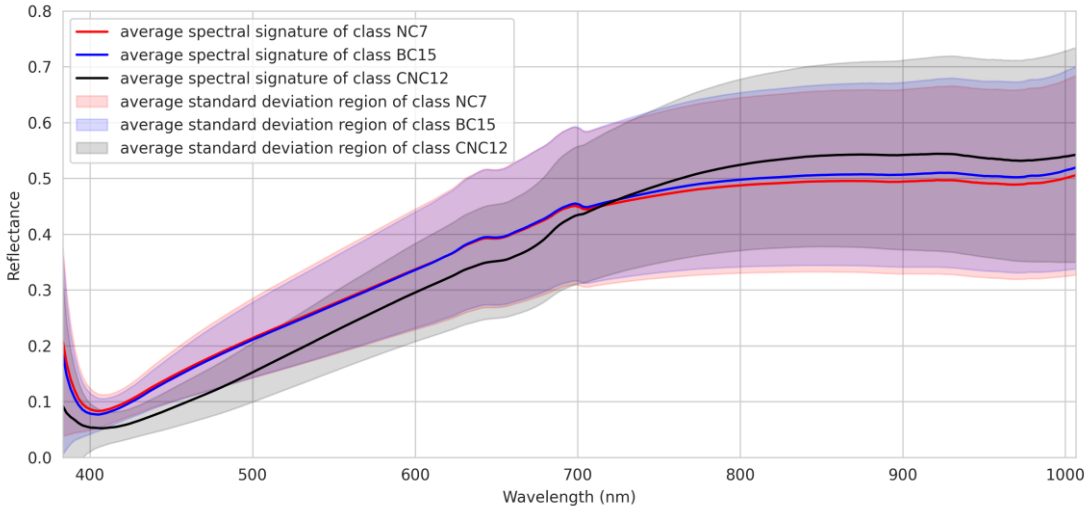

Fig. 6. Average spectral signatures and standard deviation regions of three selected seed classes. Note the great similarities between spectral information of classes NC7 and BC15, and a significant difference between them and class CNC12. Mean spectral signature and standard deviation were averaged across all 96 samples of selected classes.

The second classification scheme involves dimensionality reduction applied on all available features combined, in difference to the baseline approach described in [8], where dimensionality reduction is done only on spectral features which are then combined with the remaining six morphological features described in section II-C1. This is done because feature spaces of greater dimensionality are more likely to provide linear separability than low dimensionality spaces [14]. In high dimensional spaces it is more likely that the data from different classes will lie on some low-dimensional surfaces or subspaces, making them easier to separate. Consequentially, techniques like LDA or LDA-initiated NCA will likely perform better if the complete feature set is utilized.

The dataset is randomly split into training and test subsets, containing 85% (7344) and 15% (1296) of the original 8640 samples, respectively. The classifier parameters are estimated using k-fold cross-validation on the training subset. Classification is done using a random forest (RF) classifier set up to use 200 decision trees for the classification using only morphological features and 500 decision trees for the classification using combined feature sets.

III. Results and Analysis

Three metrics are used to evaluate classification performance, precision, recall and F1 score. Average values of these scores across all 90 classes are considered as the final classification score. The results of classification based on morphological features are given in Table I. It shows that illumination correction alone, without the addition of new features, provides noticeable improvement compared to the baseline approach described in [8].

The application of an additional set of morphological and border related features provided a significant improvement. Feature elimination using MI scores, given in Fig. 5, showed underwhelming results. RFE managed to eliminate over half of the features while slightly improving results. The full feature set combined with NCA provided the most significant improvement to the overall classification success. In comparison to the previous two methods, this technique was able to reduce the number of correlated features, but still preserve a significant part of the discriminative information shared among them.

These results suggest that there is a certain amount of redundant information provided by this set of features. However, it can also be concluded that the significance of a single feature cannot be evaluated independently and that correlation among features must be taken into consideration in the process of dimensionality reduction. Namely, the elimination of features that were estimated to be the least informative resulted in a large number of misclassifications. This indicates that features that are not informative in relation to the distribution of all 90 classes may still be important for distinguishing individual classes that cannot be correctly identified otherwise (in the domain of other, more informative features).

The results of the classification using spectral features are given in Table II. The classification using the spectral mean signature shows results that are considerably better than the classification using only morphological features, however it is not accurate enough to have a real life application in the food industry. The addition of variance has brought a noticeable improvement in results, suggesting that there is a certain amount of discriminatory information in the spectral domain that remains unused in a large number of modern approaches. This is an interesting phenomenon that can improve the results of classification in further research.

Despite the added spectral variance, there are still certain classes that show remarkable similarity in spectral characteristics. Fig. 6 shows an example of such classes, NC7 and BC15. Beside them, the CNC12 class is presented as an example of drastically different spectral characteristics. When classified on the test set using spectral mean and variance for the NC7 class, an accuracy of 60% was achieved, with 27% of the samples misclassified as BC15. With the addition of the proposed morphological feature set, these results were improved to an accuracy of 80% with only 13% of NC7 seeds classified as BC15.

The results of classification using combined morphological and spectral features are given in Table III. When using only the spectral mean features (baseline set of spectral features) combined with the morphological feature set

and dimensionality reduction approach proposed in this paper, the average F1 score increases by over 5% compared to the baseline approach. Likewise, the average F1 score is 10% higher when using the proposed feature set compared to classification using only the spectral domain. This confirms that the proposed morphological feature set provides valuable information for rice seed classification.

TABLE I. CLASSIFICATION RESULTS USING MORPHOLOGICAL FEATURES

Tested approaches	Number of features	Average results (%)		
		Precision	*Recall*	*F1 score*
baseline [8], original 6 features	6	15.94	16.09	15.82
original 6 features + lighting correction	6	17.81	17.87	17.58
proposed feature set	88	31.49	32.19	30.85
proposed feature set + elimination using MI	40	21.94	22.06	21.36
proposed feature set + elimination using RFE	40	32.76	32.68	31.68
proposed feature set + NCA	40	38.17	39.22	37.43
proposed feature set + NCA	6	20.43	21.09	20.41

TABLE II. CLASSIFICATION RESULTS USING SPECTRAL FEATURES

Tested approaches	Number of features	Average results (%)		
		Precision	*Recall*	*F1 score*
spectral mean + NCA	90	71.80	71.52	70.56
spectral variance + NCA	90	47.47	46.44	43.71
spectral mean + spectral variance + NCA	90	77.32	76.94	76.35

TABLE III. CLASSIFICATION RESULTS USING MORPHOLOGICAL AND SPECTRAL FEATURES

Tested approaches	Number of features	Average results (%)		
		Precision	*Recall*	*F1 score*
baseline [8], original 6 morphological features + spectral mean LDA	91	79.64	78.80	78.27
morphological feature set + spectral mean + NCA	90	84.33	83.75	83.43
morphological feature set + spectral mean + spectral variance + NCA	90	86.21	86.00	85.65

IV. CONCLUSION

The presented experimental study has demonstrated the significance of careful spatial features design and measured resulting improvements in the performance of rice seed varieties classification using RGB and hyperspectral images. It was confirmed that application of the proposed set of spatial features related to morphological and region border attributes of the rice seeds opens space for further performance improvements of similar seed classification systems, relying on a combination of spatial and spectral features. On the other hand, the proposed approach also includes the addition of spectral variance features to the spectral mean values regularly used in the literature. Thus, results show that the proposed feature set provides significant improvement over the existing approaches in the literature and achieves a competitive classification performance with F1 score of 85.65% on the task of classifying a large number of 90 rice seed varieties.

V. REFERENCES

[1] W. Liu, J. Liu, L. Triplett, J. Leach and G. Wang, "Novel Insights into Rice Innate Immunity Against Bacterial and Fungal Pathogens", Annual Review of Phytopathology, vol. 52, no. 1, pp. 213-241, 2014. https://doi.org/10.1146/annurev-phyto-102313-045926

[2] Z. Qiu, J. Chen, Y. Zhao, S. Zhu, Y. He and C. Zhang, "Variety Identification of Single Rice Seed Using Hyperspectral Imaging Combined with Convolutional Neural Network", Applied Sciences, vol. 8, no. 2, p. 212, 2018. https://doi.org/10.3390/app8020212

[3] K. Kiratiratanapruk, P. Temniranrat, W. Sinthupinyo, P. Prempree, K. Chaitavon, S. Porntheeraphat and A. Prasertsak, "Development of Paddy Rice Seed Classification Process using Machine Learning Techniques for Automatic Grading Machine", Journal of Sensors, vol. 2020, pp. 1-14, 2020. https://doi.org/10.1155/2020/7041310

[4] V. Truong Hoang, D. Van Hoai, T. Surinwarangkoon, H. Duong and K. Meethongjan, "A comparative study of rice variety classification based on deep learning and hand-crafted features", ECTI Transactions on Computer and Information Technology (ECTI-CIT), vol. 14, no. 1, pp. 1-10, 2020. https://doi.org/10.37936/ecti-cit.2020141.204170

[5] C. N. M. Peralta, J. P. Pabico and V. Y. Mariano, "Modeling shapes using uniform cubic B-splines for rice seed image analysis," 2016 IEEE Sixth International Conference on Communications and Electronics (ICCE), pp. 326-331, 2016, https://doi.org/10.1109/CCE.2016.7562657

[6] L. Wang, D. Liu, H. Pu, D. Sun, W. Gao and Z. Xiong, "Use of Hyperspectral Imaging to Discriminate the Variety and Quality of Rice", Food Analytical Methods, vol. 8, no. 2, pp. 515-523, 2014. https://doi.org/10.1007/s12161-014-9916-5

[7] S. Weng, P. Tang, H. Yuan, B. Guo, S. Yu, L. Huang, C. Xu, "Hyperspectral imaging for accurate determination of rice variety using a deep learning network with multi-feature fusion", Spectrochimica Acta Part A: Molecular and Biomolecular Spectroscopy, vol. 234, 2020. https://doi.org/10.1016/j.saa.2020.118237

[8] S. Fabiyi, H. Vu, C. Tachtatzis, P. Murray, D. Harle, T. Dao, I. Andonovic, J. Ren, S. Marshall, "Varietal Classification of Rice Seeds Using RGB and Hyperspectral Images", IEEE Access, vol. 8, pp. 22493-22505, 2020. https://doi.org/10.1109/access.2020.2969847

[9] H. Vu, C. Tachtatzis, P. Murray, D. Harle, T. Dao, I. Andonović, S. Marshall, S. D. Fabiyi, RGB and VIS/NIR Hyperspectral Imaging Data for 90 Rice Seed Varieties [Data set], IEEE Access, 2019. http://doi.org/10.5281/zenodo.3241923

[10] Y. Wu, S. Jiang, Z. Xu, S. Zhu and D. Cao, "Lens distortion correction based on one chessboard pattern image", Frontiers of Optoelectronics, vol. 8, no. 3, pp. 319-328, 2015. https://doi.org/10.1007/s12200-015-0453-7

[11] H. A. Rowley, "Neural Network-Based Face Detection", Ph.D., Carnegie Mellon University, 1999.

[12] R. C. Gonzalez and R. E. Woods, Digital Image Processing, 4th ed. Pearson, pp. 819-843, 2018.

[13] J. Goldberger, S. Roweis, G. Hinton and R. Salakhutdinov, "Neighbourhood Components Analysis", Advances in Neural Information Processing Systems, vol. 17, pp. 513-520, 2005.

[14] T. Cover, "Geometrical and Statistical Properties of Systems of Linear Inequalities with Applications in Pattern Recognition", IEEE Transactions on Electronic Computers, vol. -14, no. 3, pp. 326-334, 1965. https://doi.org/10.1109/pgec.1965.264137

[15] J. Burger and P. Geladi, "Hyperspectral NIR image regression part I: calibration and correction", Journal of Chemometrics, vol. 19, no. 5-7, pp. 355-363, 2005. https://doi.org/10.1002/cem.938

[16] J. Cooley and J. Tukey, "An algorithm for the machine calculation of complex Fourier series", Mathematics of Computation, vol. 19, no. 90, pp. 297-301, 1965. https://doi.org/10.1090/s0025-5718-1965-0178586-1

[17] A. Kraskov, H. Stögbauer and P. Grassberger, "Estimating mutual information", Physical Review E, vol. 69, no. 6, 2004. https://doi.org/10.1103/physreve.69.06613